Relating Tectonic Spreading Rate to Crustal Roughness across a Tectonic Triple Junction Using High-Resolution Multibeam Sonar

George Roth

School of Oceanography, University of Washington, Seattle, WA 98105

georoth@u.washington.edu

June 1st, 2012

Non-Technical Summary

Mid-ocean ridges, where magma is released to form new oceanic crust, can differ greatly in their shape depending on how quickly crust is produced and the complexity of the surrounding system of tectonic plates and plate boundaries. Several previous studies have determined an exponential relationship between the rate at which crust is formed and the physical roughness of the crust's surface. In this study, I analyze bathymetric data taken aboard the *R/V Thomas G. Thompson* during the March 2012 School of Oceanography Senior Thesis Cruise at the Pacific-Rivera mid-ocean ridge, southeast of the Baja California peninsula, and determine that here, the surrounding crust is much smoother than what the published mathematical relationship between spreading rate and roughness would lead us to expect. I discuss several possible factors that might be influencing these results, including sediments being deposited on the ocean floor, the way in which oceanic crust cools over time, stresses from nearby plate movements, and questions about the mathematical methods that I and other scientists use to derive our results. Finally, I suggest instruments and methods that might improve the accuracy of future studies on the shape and speed of mid-ocean ridge spreading.

Acknowledgements

I would like to thank the crew of the *R/V Thomas G. Thompson* for their hard work and incredible patience during the student cruise. Fellow students in the 2012 Beam Team provided survey help, analysis tips, constructive peer reviews, and constant entertainment throughout the cruise and the course. Finally, I would like to acknowledge the incredible mentorship of Dr. Miles Logsdon, whose thirst for discovery and cheerful attitude kept us all afloat in rough seas.

Abstract

The spreading rate of a mid-ocean ridge and the geomorphological roughness of the surrounding ridge flanks have shown an empirically-derived exponential relation. However, multiple worldwide spreading ridge datasets have shown large variability in crustal roughness for a given spreading rate that can range from half to twice the theoretical value. In profiles extracted from high-resolution multibeam swath bathymetry collected in March 2012 at a tectonic triple junction at the intersection of the Pacific and Rivera plates and the Tamayo transform fault near 22° N, 108° W, ridge flank roughness is significantly lower than the theoretical value expected from the known full spreading rate of ~110 mm yr^{-1}. The four profiles show calculated roughness values ranging between 27-55 meters, compared to a theoretical value of 103 meters from a global model. The variation between the expected and actual results are attributed to the influences of sediment blanketing the seafloor and draping on the sides of the flank ridges, tectonic stresses from the Tamayo transform fault, and the effects of data resolution on the calculation of roughness values. Future studies on mid-ocean ridge spreading using bathymetry from multibeam sonar will need to quantify local sedimentation and tectonic deformation in order to properly calibrate their results.

Introduction

The boundary between the Pacific and Rivera plates is an active spreading margin with half-spreading rates of 50-65 mm yr^{-1}. (DeMets and Wilson 1997; DeMets et al. 2010; Bandy et al. 2010) Forming a triple junction from the northernmost edge of this boundary is the Tamayo Transform, which incurs a counterclockwise torque on the Rivera plate. This tectonic stress can be observed in large-scale bathymetric data (Smith and Sandwell, 1997) as horizontal

deformation at the triple junction site. Intensity returns from multibeam surveys conducted 300-400 km farther south along the main Rivera Transform and Moctezuma Spreading Segment have shown additional irregularities in ridge orientation and sedimentation in this tectonic setting. (Bandy et al. 2008)

In model studies linking morphology at the ridge axis to ridge spreading rate, Phipps Morgan and Chen (1993) determined that axial valleys and steep, frequent ridge topography result from a sporadic, non-steady-state magma lens, which in turn produces slow half-spreading rates below 20 mm yr^{-1}. Ridges with faster half-spreading rates, such as the East Pacific Rise (50 mm $yr^{-1}$and higher) , show sharp axial highs with relatively smoother topography with increasing distance from the ridge axis, produced by constant magma supply from a steady-state magma chamber.

Malinverno (1991) examined dozens of spreading ridges and related their spreading rates (derived from magnetic anomaly data) to their geomorphic roughness. To calculate roughness for a one-dimensional profile across a spreading ridge, Malinverno used a residual root mean square method, defined as the standard deviation of the residual topography about a linear trend:

$$R_i = \sqrt{\sum_{i=1}^{n} \frac{h_i^2}{n}}$$

where R_i is RMS roughness, in units of meters, *h* is the difference between the measured depth at a point and the linear trend, and *n* is the total number of sample points that make up the specified linear profile. Finally, a logarithmic trend line was fit to a plot of roughness vs. spreading rate over a hundred profiles over oceanic spreading ridges:

$$R = 1296v^{-0.539}$$

where *R* is the theoretical roughness value and *v* is the ridge's full spreading rate in mm yr^{-1}.

Oceanic crust becomes denser with age when newly-formed crust cools both from heat flux to the ocean and with increasing distance from the hot volcanic spreading center. This increasing density causes the crust to subside, and the depth of subsidence is calculated in a linear relationship with the square root of crustal age. In order to account for this deep tectonic process, calculations of residual topography should be normalized to this subsidence curve, rather than a linear fit.

Several studies (Bird and Pockalny 1994; Hauschild et al. 2003; Whittaker et al. 2008; Ehlers and Jokat 2009) have examined the spreading rate-roughness relation in ultra-slow, slow, and fast-spreading ridges and observed noticeable variability within the general agreement. The Pacific-Rivera-Tamayo triple junction (Fig. 1), located near 22° N, 108° W, is an "intermediate" spreading ridge, with a half-spreading rate averaging 55 mm yr^{-1}. (DeMets and Wilson 1997; DeMets et al. 2010; Bandy et al. 2010) Intermediate spreading ridges often exhibit geomorphology that is not entirely consistent either slow- or fast-spreading ridges. This makes the triple junction an ideal candidate to further examine roughness variability by taking into account its non-uniform orientation and morphology.

Here, I hypothesized that crustal roughness at this spreading ridge would match the value inferred from its measured spreading rate following the Malinverno (1991) model. Variability from the idealized roughness values may then be attributed to geological and technological factors and processes unique to this region.

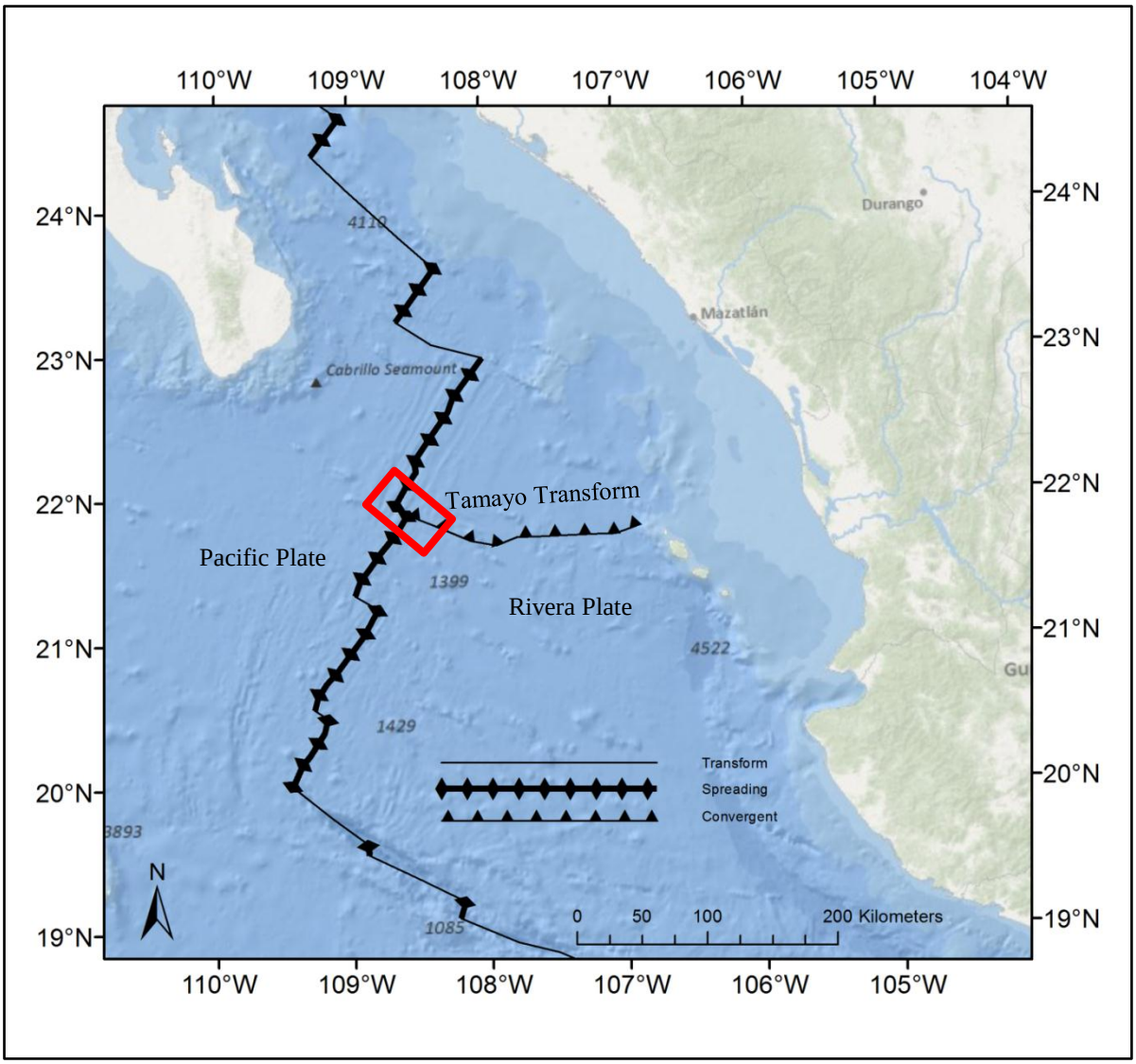

Figure 1: Map of the tectonic setting at the Pacific-Rivera-Tamayo triple junction, and the study area, outlined in red.

Methods

The bathymetric survey in this study (Fig. 2) was conducted during March 2012 as part of the University of Washington's School of Oceanography senior thesis cruise from San Diego, California to Manzanillo, Mexico aboard the *R/V Thomas G. Thompson*. The multibeam sonar device was a Kongsberg EM302. Real-time parameters such as ship roll, pitch, heave, and water column sound velocity were used to automatically calibrate the data in Kongsberg SIS software to prepare the data for import and analysis.

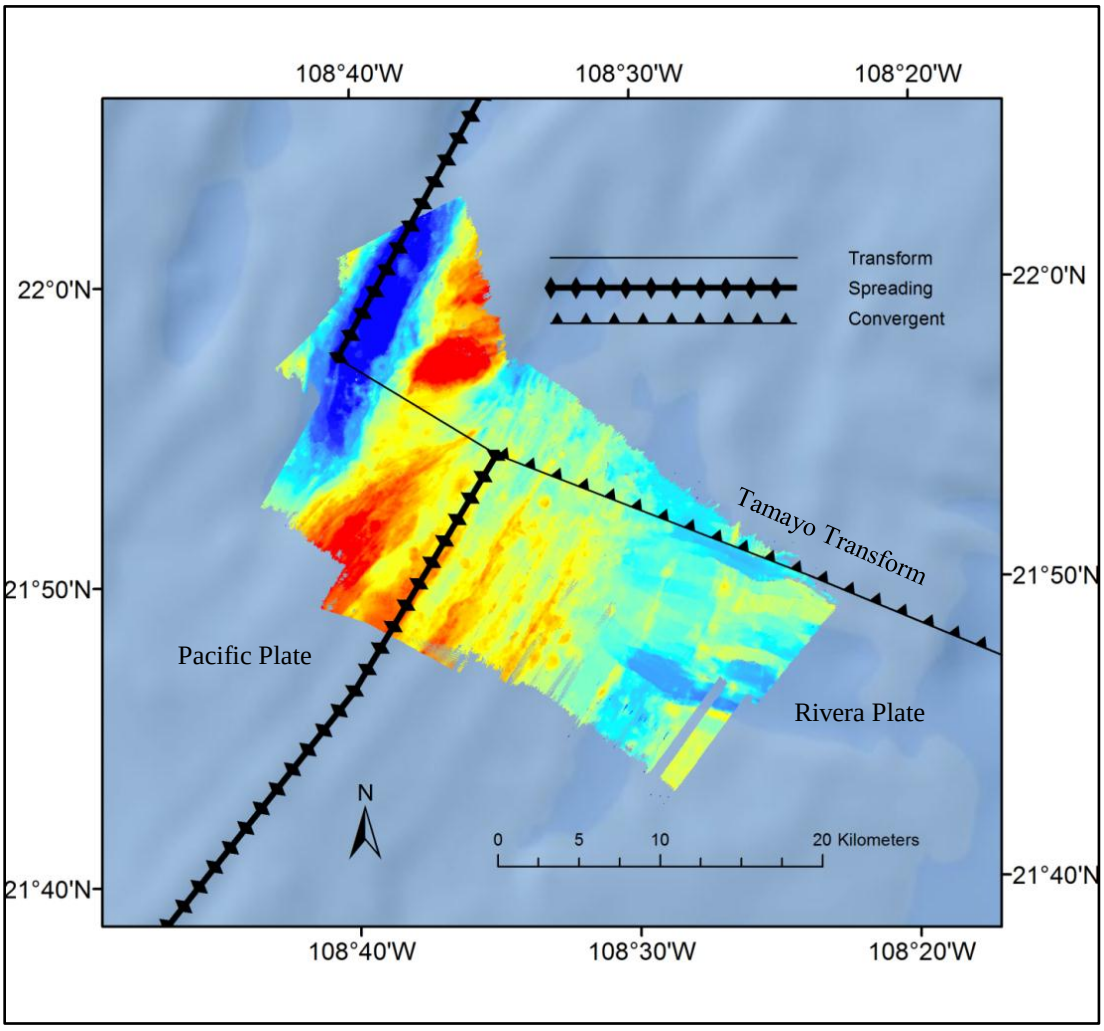

Figure 2. Two-dimensional view of the cleaned bathymetric data surface and its tectonic setting. Warmer colors are shallower.

I then imported the raw data lines into Caris HIPS and SIPS post-processing software, excluding areas that contained poor quality data from mapping during turns and data that was outside my study area. I then ran the CUBE (Combined Uncertainty and Bathymetry Estimator) algorithm as an operation within HIPS and SIPS, which cleaned the data surface by eliminating points with depths that were local statistical outliers, making an estimate of the depth at a given location based on hypotheses developed from the combination of the density and local variation about each location. The CUBE algorithm produced cleaned surfaces at four user-defined resolutions (due to time constraints) of 10, 20, 50, and 100 meters to facilitate comparison between the results of different data resolutions. The 10 meter surface was rejected from analysis because of numerous gaps in the data – artifacts of the low horizontal and vertical resolutions the sonar can resolve at ~3000 meter depths, and because any attempt to interpolate the space between the points would invalidate roughness calculations. No tide or sound velocity corrections were applied to the surface, both because these signals would not propagate significantly enough to affect the vertical depth estimates at the sonar's resolution at this depth, and because roughness is a measure of local variance rather than absolute location over a large scale.

Finally, I converted the cleaned surfaces first to a universal ASCII format and then to ESRI's proprietary GRID raster format for analysis in ESRI ArcMap 10. I imported a shapefile of tectonic boundaries provided by the US Geological Survey (2012), and, for the purposes of this study, interpreted the plate boundary line as the morphological ridge axis. I established four spatial profile lines (labeled A, B, C, and D) perpendicular to the ridge axis at a distance of 3 km from each other, which provided even spacing and placement within overlapping survey

transects. Each profile was drawn to an extent of approximately 16.5 km each (Fig. 3), the maximum that could be drawn without intersecting any gaps in the data.

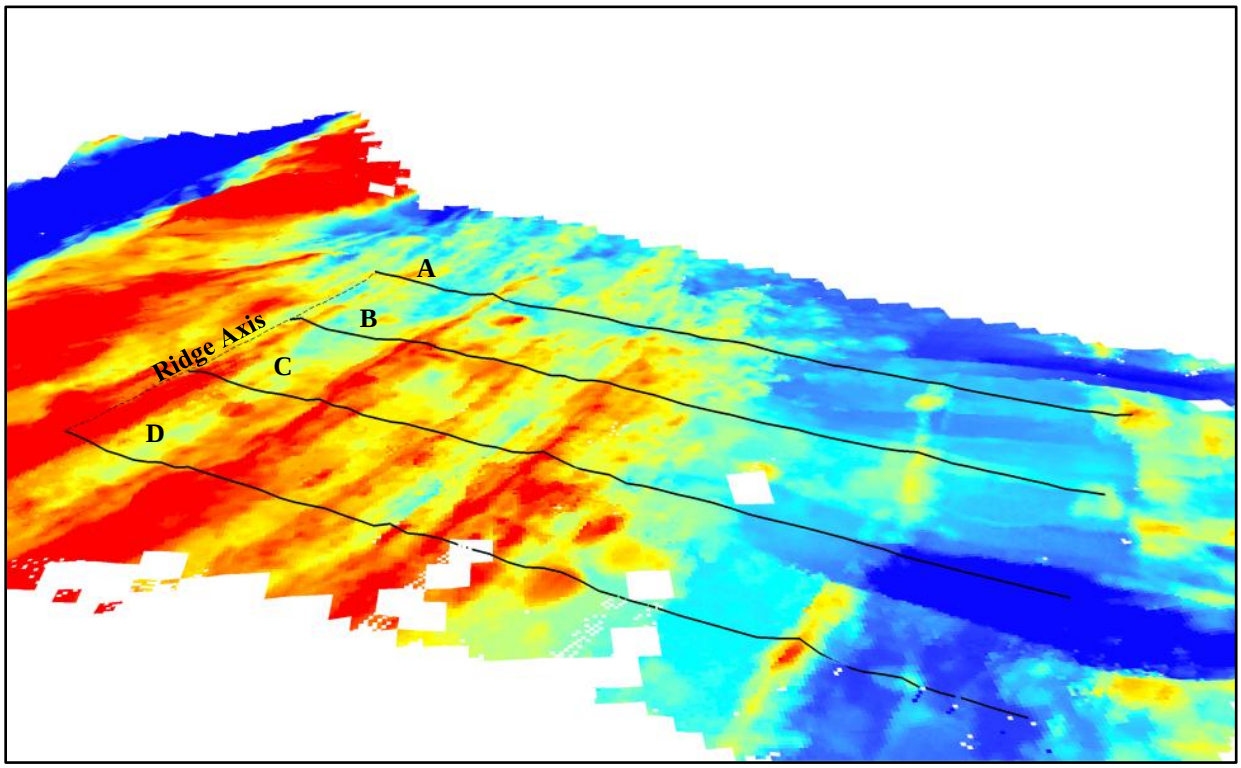

Figure 3. Three-dimensional view of the cleaned bathymetric data surface, ridge axis, and the four analysis profiles.

Bathymetric depths were extracted along the profile lines (Fig. 4) from the 20, 50, and 100 meter surfaces and the extracted data imported into Microsoft Excel. To calculate root mean square (RMS) roughness, I created a linear regression through each of the profiles, then summed the variances of each profile point from the linear regression and took the square root of each sum, following the Malinverno (1991) equation.

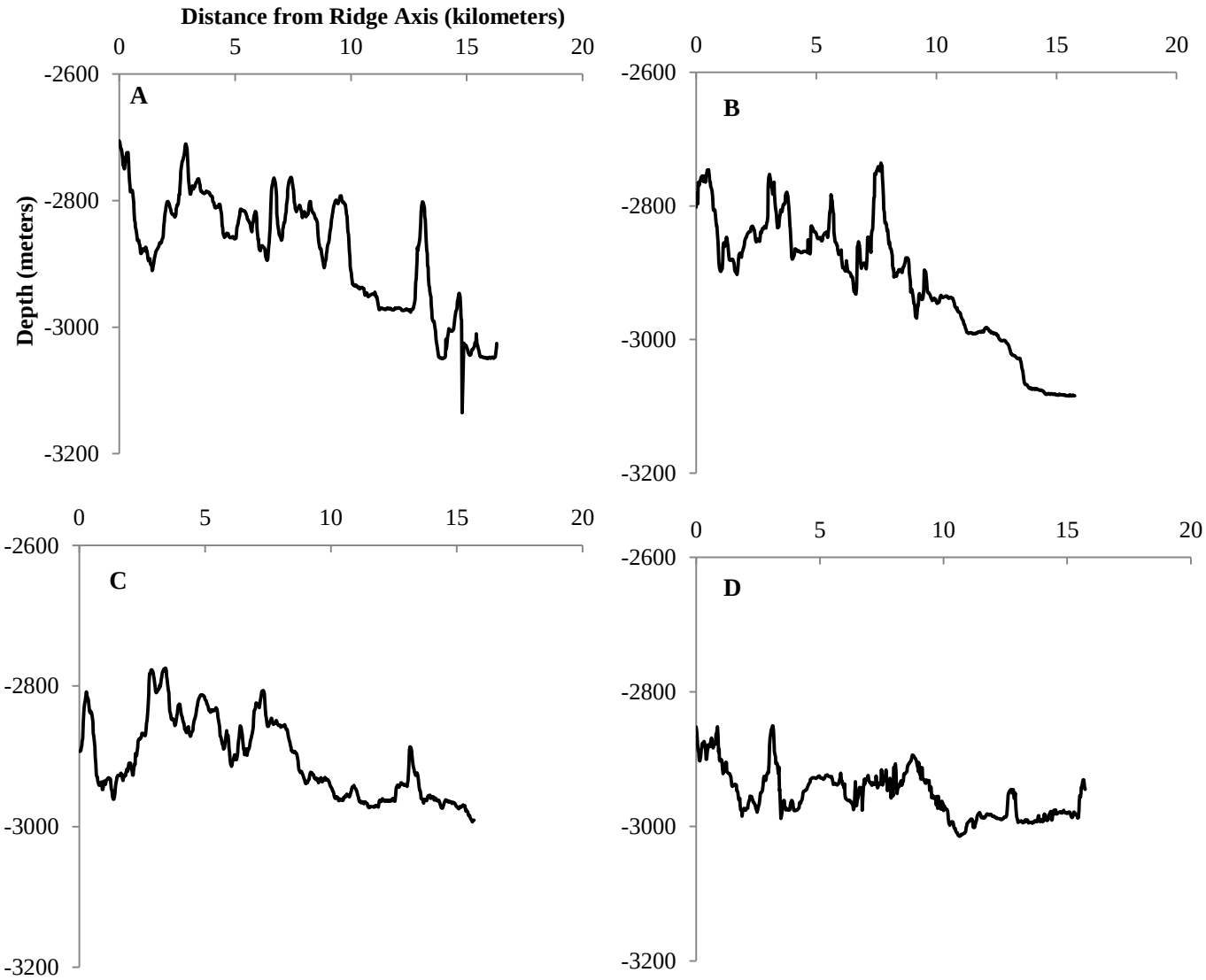

Figure 4. The four bathymetric profiles with distance from the ridge axis, using depth values extracted from the 20 meter bathymetric surface.

Results

The root mean square (RMS) roughness values for each profile are presented in Table 1, and range from 27 meters for profile D to 55 meters for profile A. The values were consistently one half to one third of the estimated value of 103 meters for a ridge with a full spreading rate of 110 mm yr^{-1}estimated using the Malinverno relation $R=1296v^{-0.539}$ (Fig. 5). Profiles B and C had lower roughness values than Profile A, and Profile D, in turn, had the lowest roughness value. The effects of raster resolution on roughness values along the same profiles (Table 1) were negligible.

Table 1

Profile	R100	R50	R20	Rm
A	53.93	54.96	55.48	102.87
B	40.58	43.13	44.66	102.87
C	41.44	41.70	42.59	102.87
D	29.98	29.03	27.18	102.87

Table 1. Columns R100, R50, and R20 represent RMS roughness results in each of the four profiles at 100, 50, and 20 meter resolutions, respectively. Rm is the theoretical roughness from the Malinverno equation for a half spreading rate of 55 mm yr^{-1}. Note that all observed roughness values are lower than the modeled values.

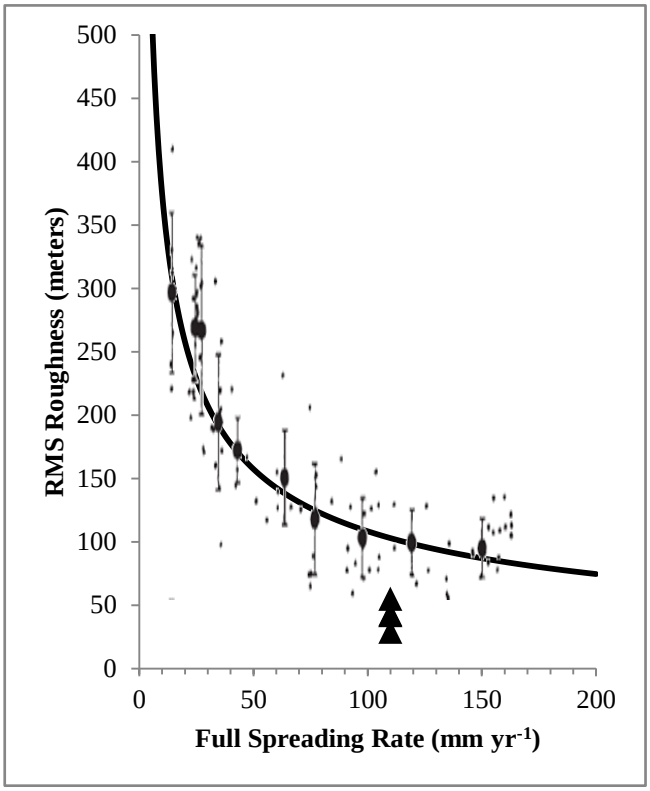

Figure 5. The Malinverno rate-roughness equation(black line) superimposed with the full results from Malinverno (1991) Results from this study (triangles) have lower RMS roughness values than all other points from Malinverno for their spreading rate

Discussion

For the spreading rates present here, the roughness results were lower than both the idealized equation and the lowest bounds of the data plotted in Malinverno (1991) as well as the synthesis data plotted in Ehlers and Jokat (2009). A number of geological and methodological factors can account for this difference.

Prior studies on the spreading rate-roughness relation have used seismic profiles to subtract the sediment layer (Bird and Pockalny 1994; Hauschild et al. 2003; Ehlers and Jokat 2009; Bartolomé et al. 2010). Conceptually, a sediment layer would tend to "smooth out" the bottom, decreasing a profile's average variance from a trend line. Hauschild et al. (2003) demonstrated that sediments at spreading ridges along the East Pacific Rise tend to "drape" along the sides of ridges, rather than "pool" in troughs. Pooling in troughs would affect a minor change in average variance, though it would serve mostly to "raise" the linear trendline to a mean shallower position. By draping on the sides of ridges, sediment will tend to decrease the slopes between peaks and troughs. Conceptually, a histogram of variances in an extremely rough surface (one that quickly oscillates between high and low topography) would produce a bimodal distribution with each mode centered on the most common high and low elevations, respectively. This same histogram for a smoother surface would move toward a normal (single-mode) distribution centered on a variance of 0. (Fig. 6)

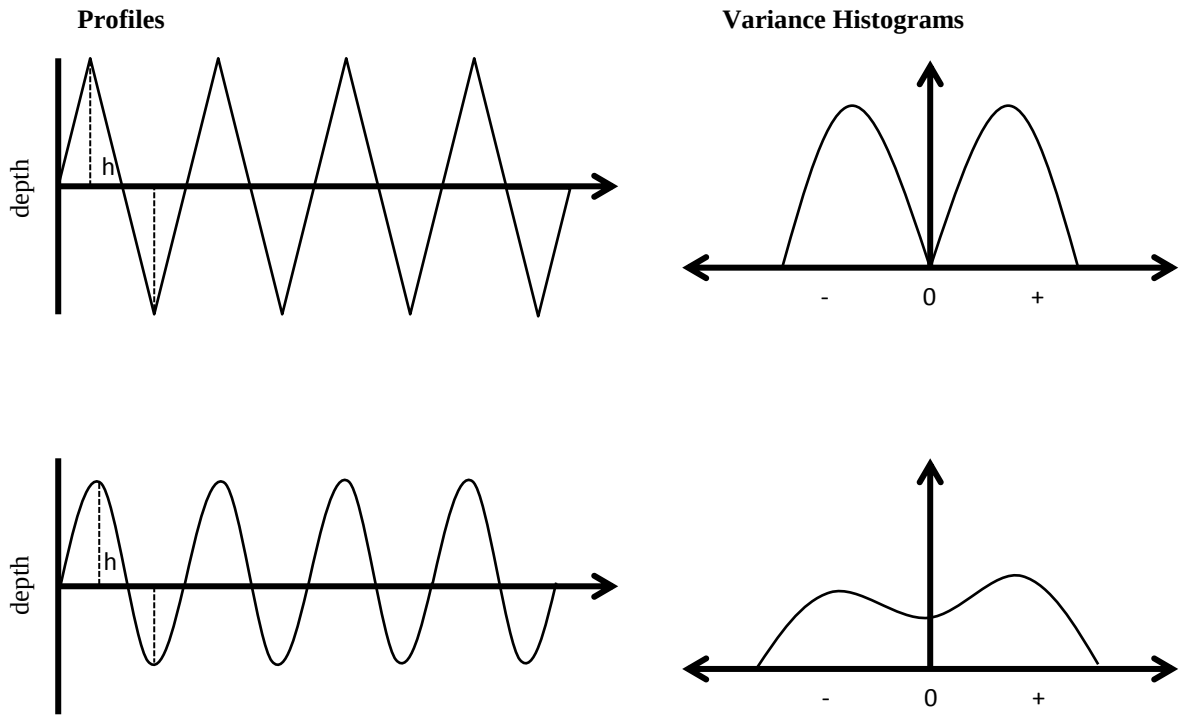

Figure 6. Conceptual diagram illustrating the effects of sediment draping on residual topographic variance across a profile. Left-side panels are conceptual profiles of a rough (top left) and smooth (bottom left) ridge series. The value "h" represents the residual variance at a given point elevation on the seafloor from a linear trend line through the entire measured profile. Histograms (right-side panels) show the conceptual distribution of h (variance) values above and below the trend (0). For the "rough" profile (top right), the distribution of variance is bimodal and centered on large values away from the trendline. For a profile smoothed by sediment draping (bottom right), the distributions of variance "flatten out" as more of the variances are measured as smaller and closer to the trend line. Conceptually, an ideally "smooth" surface measured at high resolution precisely follows the trend in topography at a much lower resolution, whereas a "rough" surface has, at a given point measurement, high variance from the low-resolution trend.

Though no studies on sedimentation rate have been conducted within this study area, qualitative interpretation of the acoustic intensity returns from the multibeam sonar data indicates a significant "softening" of the ocean floor farther out from the ridge axis. Though this study site was over 150 km from the nearest coastline and on average more than 2700 m deep, it remains possible that, due to the Pacific-Rivera spreading ridge's proximity to upwelling-driven biology at the coast of Mexico, it may receive higher sedimentation than at a standard, mid-ocean abyssal location.

Bird and Pockalny (1994) illustrated the significant effect of a sediment layer in contrasting seafloor and basement crust roughness. (Fig. 7) Though their data are from the South Australian and Argentine Basins, they provide a useful starting point for bracketing the possible thickness of a sediment layer that could account for the variation in my study's results. For example, a thinner, 50 meter layer in Bird and Pockalny's data represents a seafloor-to-basement roughness ratio of 0.8. For the results here at the Pacific-Rivera-Tamayo junction, this ratio would produce a basement roughness of 34-69 m, somewhat closer to Malinverno's results. To account for the total difference between the average of my results and the idealized curve using Bird and Pockalny's data, a seafloor/basement roughness ratio of approximately 0.4 is needed, and could account for a sediment layer up to 800 m thick. Though sedimentation can clearly produce incredibly large variation in seafloor roughness, the link between the two in the literature is highly variable and should not be interpreted as a first-order control.

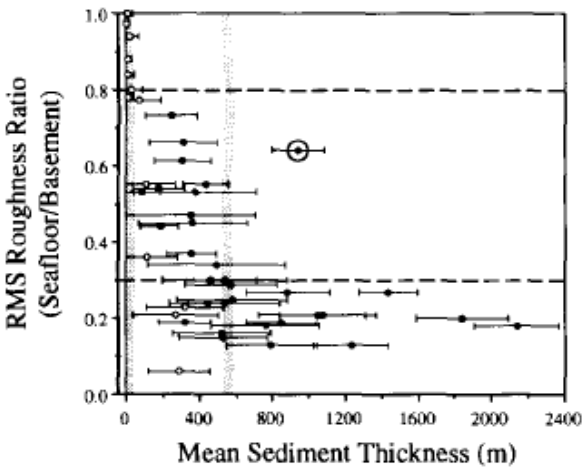

Figure 7. The effects of sedimentation on RMS roughness.

Figure and caption reprinted from Fig. 9 of Bird and Pockalny (1994, Earth and Planetary Science Letters**).**

Crustal age (top) and RMS roughness ratio (ratio of seafloor RMS roughness to basement RMS roughness, bottom) plotted versus mean sediment thickness from single-channel seismic data. Horizontal bars are standard deviations for sediment thickness and vertical bars are age ranges for each sample profile. Vertical patterned lines separate three regions of the bottom plot based on mean sediment thicknesses of less than 50 m, 50-550 m, and greater than 550 m (see text). Horizontal dashed lines correspond to roughness ratios of 0.3 (seafloor roughness is 30% of measured base- ment roughness) and 0.8 (seafloor roughness is 80% of basement roughness). Encircled data value is an outlier. Sediments do not necessarily thicken monotonically with increasing crustal age. Oceanic basement is smoothed substantially if covered by sediments greater than 50 m thick (on average)

Malinverno (1991) remarked that mantle temperature and distance from transform faults may be responsible for the variation in assembled data. Whittaker et al. (2008) examined regions of older, Cretaceous crust on a global scale, and removed both the spreading rate- and sedimentation-influenced roughness signals. This exposed a remaining signal that they interpreted as originating from a spreading ridge with a different geographic configuration and temperature profile than present-day spreading ridges. However, at the Pacific-Rivera spreading ridge, with an average spreading rate of 55 mm yr^{-1}, the 16.5 km profiles reach a maximum crustal age of 300 kYa, which is too young for any significant tectonic rearrangement.

Because the Pacific-Rivera plate boundary is considered an "intermediate" spreading ridge (40-90 mm yr^{-1}), several characteristics present in both slow- and fast-spreading ridges may influence the topographic roughness. (Whittaker et al., 2008) Outside the immediate study area, an overlapping spreading center is observed, and the migration of this overlapping region along the ridge axis can be responsible for propagated variation in both the topography and orientation of older crust farther from the ridge axis.

The residual variance was normalized to account for subsidence by first calculating the curve (Fig. 8), where subsidence depth is a function of crustal age, derived from spreading rate and profile distance, and then using it as the "mean" line, rather than the linear regression. For Profile B over the 20 meter raster, the RMS roughness increased modestly from 44.66 to 53.94 using this method. Despite the exponential decrease in slope magnitude with profile distance, the subsidence method also did not appear to preferentially designate any large regions as "rougher" or "smoother" compared to the linear method. (Fig. 9) If spreading rates near a particular ridge segment are known, then roughness metrics can be quickly and easily calibrated for crustal subsidence.

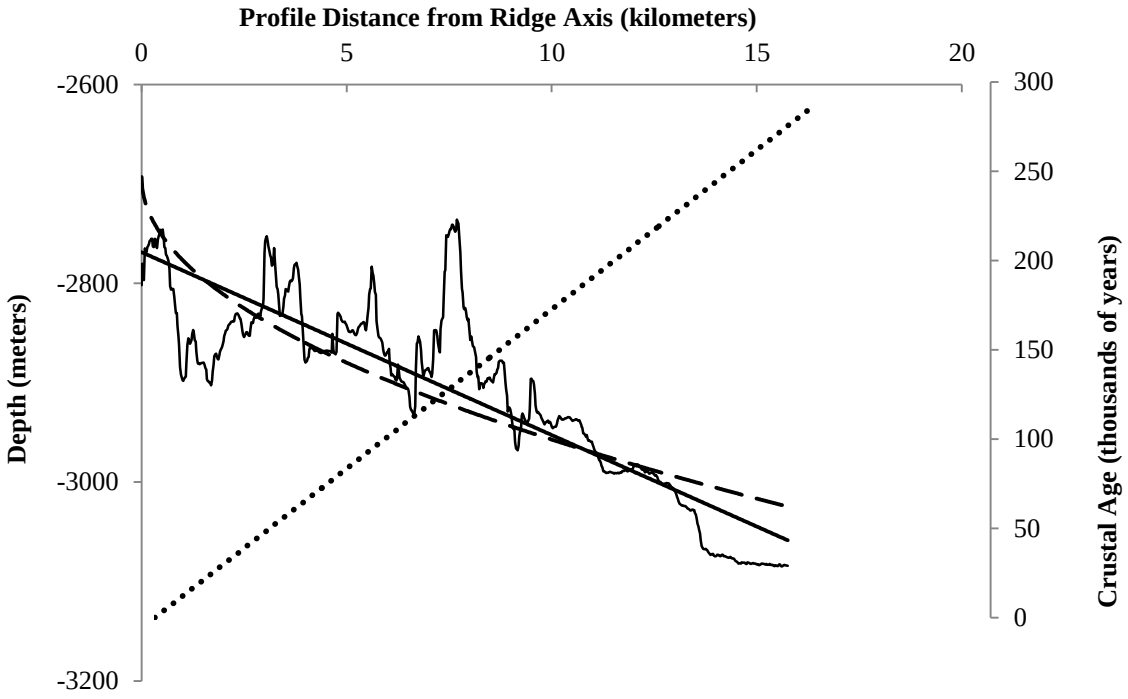

Figure 8. Metrics from Profile B, showing crustal age with distance calculated from the 55 mm yr^{-1} half spreading rate (dotted line), a linear regression of depth (solid line), and the corrected age-subsidence curve (dashed line).

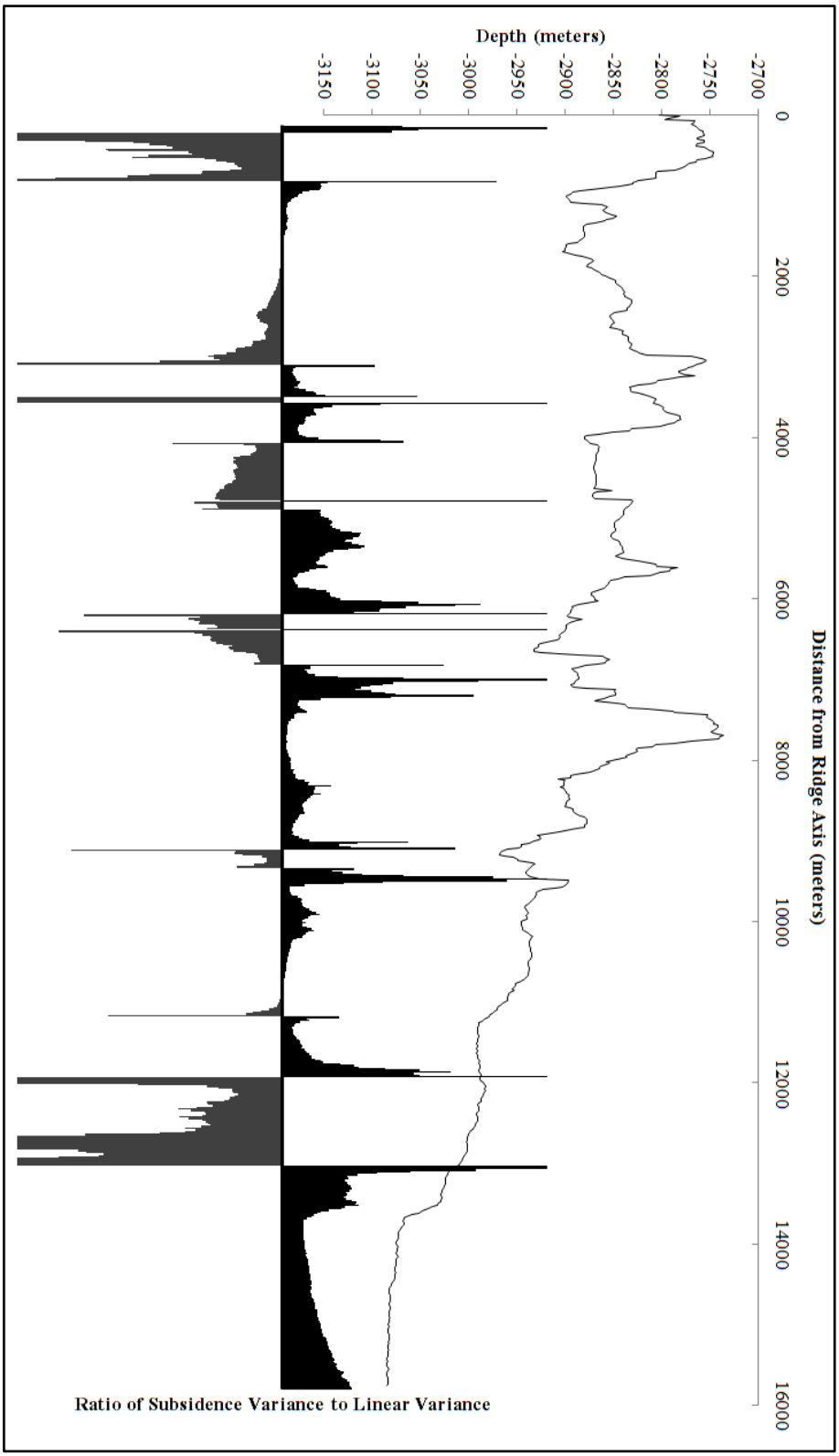

Figure 9. Profile A (solid line), superimposed with a dimensionless ratio (black and grey) demonstrating the subsidence curve over- or under-estimating variance relative to a linear fit.

Though Malinverno (1991) analyzed profiles ranging from 500-1000 km long and with a low sampling resolution of 2.5 km, others (Bird and Pockalny, 1994; Ehlers and Jokat, 2009) have demonstrated comparable results in similar analyses with profiles on the order of tens of kilometers with higher sampling resolutions.

In the Density and Locale setting used in the CUBE algorithm used to initially clean the dataset, topographic variation at scales smaller than 20 meters may have been partially eliminated, due to the way the algorithm produces a bathymetric estimate for a given X, Y location by analyzing the residual depth uncertainty in a data cloud of bathymetric soundings. However, the variance metric at each point in the summed RMS roughness calculation divides by the total number of sample points, which effectively prevents the roughness calculation from being greatly affected by raster resolution. Though there may be a greater number of small-scale variances present in the 20 meter-resolution profile, the number of sample points is five times the number in the 100 meter profile. However, it is conceivable that drastically finer or coarser horizontal resolutions compared to the scale of the ridge features and their variability would produce significantly different results. The multibeam sonar was unable resolve detail below a resolution of about 20 meters, but an extremely coarse resolution of 1 km or greater would fail to capture the topographic variability and would produce a less accurate roughness estimate. This has implications for performing similar analyses on global, coarser datasets, such as those derived from satellite-observed gravity anomalies. (Smith and Sandwell, 1997)

Conclusions

Bathymetric profiles demonstrated flank roughness is significantly lower than expected from the known spreading rate of ~110 mm yr^{-1}. The four profiles show calculated roughness values ranging between 27-55 meters, compared to an idealized value of 103 meters, and grew smoother with distance from the triple junction. The effects of sediment draping on the sides of the flank ridges, tectonic stresses from the Tamayo transform, and data resolution on the derived roughness values may contribute to the inconsistency between the modeled values and observed data. Correcting for crustal subsidence also appears to lend better context to the roughness values and eases comparisons between unconnected spreading ridges by normalizing for a universal and dynamic geological process.

Though the observed roughness results here were significantly lower than the idealized Malinverno curve, further data is needed to decisively determine whether the sedimentation or the tectonic factors are responsible for the major variation. Previous studies on crustal roughness used seismic reflection profiles to resolve sediment thickness. Future studies on mid-ocean ridge spreading using bathymetry from multibeam sonar will first need to quantify local sedimentation and tectonic deformation in order to properly calibrate their results.

References

Bandy, W. L., F. Michaud, J. Dyment, C. a. Mortera-Gutiérrez, J. Bourgois, T. Calmus, M. Sosson, J. Ortega-Ramirez, J.-Y. Royer, B. Pontoise, and B. Sichler. 2008. Multibeam bathymetry and sidescan imaging of the Rivera Transform–Moctezuma Spreading Segment junction, northern East Pacific Rise: New constraints on Rivera–Pacific relative plate motion. Tectonophysics **454**: 70-85, doi:10.1016/j.tecto.2008.04.013

Bandy, W. L., F. Michaud, C. a. Mortera Gutiérrez, J. Dyment, J. Bourgois, J.-Y. Royer, T. Calmus, M. Sosson, and J. Ortega-Ramirez. 2010. The Mid-Rivera-Transform Discordance: Morphology and Tectonic Development. Pure and Applied Geophysics **168**: 1391-1413, doi:10.1007/s00024-010-0208-8

Bartolomé, R., J. Dañobeitia, F. Michaud, D. Córdoba, and L. a. Delgado-Argote. 2010. Imaging the Seismic Crustal Structure of the Western Mexican Margin between 19°N and 21°N. Pure and Applied Geophysics **168**: 1373-1389, doi:10.1007/s00024-010-0206-x

Bird, R. T., and R. A. Pockalny. 1994. Late Cretaceous and Cenozoic seafloor and oceanic basement roughness: Spreading rate, crustal age and sediment thickness correlations. Earth and Planetary Science Letters **123**: 239-254.

Calder, B., and D. Wells. 2007. CUBE User's Manual, Version 1.13. Center for Coastal and Ocean Mapping and NOAA/UNH Joint Hydrographic Center, University of New Hampshire. http://ccom.unh.edu/sites/default/files/publications/Calder_07_CUBE_User_Manual.pdf, Retrieved on May 28th, 2012.

DeMets, C., R. G. Gordon, and D. F. Argus. 2010. Geologically current plate motions. Geophysical Journal International **181**: 1-80, doi:10.1111/j.1365-246X.2009.04491.x

DeMets, C., and D. S. Wilson. 1997. Relative motions of the Pacific, Rivera, North American, and Cocos plates since 0.78 Ma. Journal of Geophysical Research **102**: 2789-2806.

Ehlers, B.-M., and W. Jokat. 2009. Subsidence and crustal roughness of ultra-slow spreading ridges in the northern North Atlantic and the Arctic Ocean. Geophysical Journal International **177**: 451-462, doi:10.1111/j.1365-246X.2009.04078.x

Hauschild, J., I. Grevemeyer, and N. Kaul. 2003. Asymmetric sedimentation on young ocean floor at the East Pacific Rise , 15 S. Marine Geology **193**: 49-59.

Malinverno, A. 1991. Inverse square-root dependence of mid-ocean ridge flank roughness on spreading rate. Nature **352**: 58-60.

Smith, W. H. F., and D. T. Sandwell. 1997. Global seafloor topography from satellite altimetry and ship depth soundings. Science **277**: 1957-1962.

United States Geological Survey. 2012. Plate Boundaries. http://earthquake.usgs.gov/regional/nca/virtualtour/kml/plateboundaries.kmz, Retrieved on January 22nd, 2012.

Whittaker, J. M., R. D. Müller, W. R. Roest, P. Wessel, and W. H. F. Smith. 2008. How supercontinents and superoceans affect seafloor roughness. Nature **456**: 938-41, doi:10.1038/nature07573